PRIFYSGOL
ABERYSTWYTH
UNIVERSITY

# Aberystwyth University

*Toward a dynamic representation of hydrological connectivity at the hillslope scale in semiarid areas*

Smith, Mark W.; Bracken, Louise J.; Cox, Nicholas J.

# Toward a dynamic representation of hydrological connectivity at the hillslope scale in semiarid areas

Mark W. Smith,[1] Louise J. Bracken,[2] and Nicholas J. Cox[2]

[1]   Hydrological connectivity has emerged as an effective means to understand and manage fluxes of water and transport of nutrients and sediment at the catchment scale, especially as fluxes are modified by changing climate and land use. However, hydrology has not yet adopted it as a unifying concept given uncertainties regarding different conceptions and gaps in understanding of how connectivity functions at different temporal and spatial scales. This paper outlines a conceptual model of hydrological connectivity for semiarid hillslopes and highlights the direction that future attempts to quantify dynamic hydrological connectivity might take. Rainfall-runoff analysis emphasizes the influence of antecedent moisture and temporal storm structure on hillslope-scale flood generation. Plot-scale field flume experiments demonstrate the spatial and temporal variability of flow resistance. The morphological runoff zone framework is presented as a method to upscale such results to the hillslope and incorporate the broader-scale issue of hillslope form. The need to design field experiments to inform attempts to model feedbacks between runoff depth and flow resistance forms the central argument of this paper. Patterns of infiltration and resistance across entire flow paths and their variability throughout a storm event are the key to understanding dynamic hydrological connectivity at the hillslope scale.

## 1.   Introduction

[2]   Hydrological connectivity is emerging as a crucial concept, enhancing understanding of the impact of heterogeneities on hydrological and geomorphological processes operating within river catchments [*Western et al.*, 2001; *Grayson et al.*, 2002; *Lane et al.*, 2004; *Troch et al.*, 2009] and bringing together researchers from a variety of disciplines [*Tetzlaff et al.*, 2007]. Recent attempts to formalize this organizing framework [e.g., *Bracken and Croke*, 2007] have identified distinct elements in semiarid hydrology (structural and functional connectivity), usefully highlighting the inadequacies of many existing research strategies.

[3]   Structural (or *static*) connectivity is the subject of most studies of hydrological connectivity and refers to spatial patterns in the landscape and the extent of physical connectedness of landscape elements. For hillslopes and channels to produce floods, runoff-generating areas must be spatially connected to the main channel network; otherwise the outflow from isolated runoff-generating areas may be reinfiltrated. *Ambroise* [2004] makes this distinction between "active" runoff-generating areas and "contributing" areas that generate runoff and are spatially connected to the channel network. There are numerous methods of identifying such

structural connectivity by classifying landscapes and catchments according to hydrological response. The hydrological runoff units (HRUs) of *Flügel* [1995] and subsequent variants [e.g., *Sharma et al.*, 1996; *Karvonen et al.*, 1999; *Bull et al.*, 2003; *Devito et al.*, 2005] divide the landscape into discrete units on the basis of a number of variables (e.g., soil type, land use). At a smaller scale, *Mueller et al.* [2007] investigated different parameter scaling tools for representing the variability of the Darcy-Weisbach friction factor and saturated hydraulic conductivity in a kinematic wave overland flow model over small semiarid catchments. This modeling experiment demonstrated the importance of representing both the spatial variation of resistance and infiltration and the spatial pattern of their connectivity.

[4]   Yet connectivity can also be understood in terms of the *processes* linking connected areas. Such linkages can strengthen or weaken over time (switching between states of coupling [*Brunsden*, 1993]). During a flood event, the strength of a runoff delivery pathway is dependent upon the water supply from upslope, yet the position of a storm cell and the temporal structure of rainfall intensity determine which flow paths become activated and when. Hydrological connectivity is therefore a dynamic property that describes the interconnection of areas by a process (*functional* connectivity [*Turnbull et al.*, 2008]). The expansion of active runoff-generating areas may eventually establish a connection with the flow network during a "contributing period" [*Ambroise*, 2004].

[5]   Much research has been conducted in temperate environments examining the heterogeneity and connectivity of subsurface flow pathways as a possible explanation

[1]Institute of Geography and Earth Sciences, Aberystwyth University, Aberystwyth, UK.
[2]Department of Geography, Durham University, Durham, UK.

for threshold behavior observed in hillslope drainage [e.g., *Western et al.*, 2001; *Sidle et al.*, 2001; *Hopp and McDonnell*, 2009] applying connectivity statistics derived from percolation theory [e.g., *Lehmann et al.*, 2007; *Di Domenico et al.*, 2007]. *Tromp-van Meerveld and McDonnell* [2006] suggest that the spatial pattern of active flow pathways is the key to conceptualizing the nonlinear process of subsurface stormflows. However, in semiarid areas with a large annual water deficit, water redistribution and horizontal fluxes are dominated by overland flows; subsurface flows provide a negligible contribution to outflows. Hortonian runoff generation in semiarid catchments is typically nonuniform and develops in isolated patches; such surface flow connections are infrequently established. There are many parallels with the subsurface threshold processes identified in the work of *Tromp-van Meerveld and McDonnell* [2006]; semiarid surface runoff development may eventually provide an accessible and analogous process for further testing and developing such connectivity statistics.

[6] Structural and functional connectivity interact to determine the dynamic and nonlinear behavior of a hydrological system (*dynamic* connectivity [*Bracken and Croke*, 2007]). Understanding of this interaction is extremely limited as most studies have focused on structural connectivity. Dynamic hydrological connectivity encompasses both short-term variation in antecedent conditions and rainfall inputs that result in nonlinear hillslope response to rainfall and longer-term landscape development (including feedbacks between runoff transfer and topographic form through erosion and deposition). *Fitzjohn et al.* [1998] and *Di Domenico et al.* [2007] identify critical points where soil moisture patterns transition from a disorganized to an organized state and structural connectivity (spatial arrangement of low abstraction potentials) ceases to influence functional connectivity (runoff transfer). *Cammeraat* [2004] also observed expanding contributing areas during a rainfall event on a semiarid hillslope. This expansion was determined not by saturation but by linkage of areas of overland flow [see also *Gomi et al.*, 2008].

[7] Such dynamic aspects of connectivity are difficult to quantify, yet models of hillslope hydrology must be able to represent these processes [*Antoine et al.*, 2009]. For a fully quantitative approach to dynamic connectivity, each influencing factor must be identified and their interactions understood. These factors include rainfall characteristics, flow path length and integration, spatial distribution of areas of low/high abstraction potential and the routing velocity of overland flows.

[8] Rainfall events in semiarid environments are often characterized by a few relatively short-lived, high-intensity bursts of rainfall with restricted spatial coverage. Many authors argue that rainfall intensity is important in the production of runoff [e.g., *Costa*, 1987; *Schick*, 1988; *Cammeraat*, 2004] whereas others emphasize the intensity-duration relationship of storms [*Yair and Raz-Yassif*, 2004] or total storm rainfall [*Bracken et al.*, 2008]. The temporal variation of rainfall intensity, including the location of intense "pulses" within the rainfall time series of a storm event, is crucial when considering the development of hydrological connections [*van de Giesen et al.*, 2000; *Wainwright and Parsons*, 2002], and so soil moisture and total storm rainfall are also influential factors.

[9] *Reaney et al.* [2007] found that travel distances of overland flow are strongly influenced by the relationship between rainfall intensity and vertical abstractions and the fragmentation of periods of high-intensity rainfall (whenever pulses are shorter than the travel time of overland flow, the runoff may infiltrate further downslope). Given this limited "travel opportunity time," surface flow resistance and routing velocity will affect not only the timing and shape of stream hydrographs but also the flood magnitude. This paper argues that the spatial and temporal variation of *both* vertical abstractions (infiltration) and horizontal transfers (flow resistance) are crucial to this process, yet only the former receives a thorough treatment in hydrological models. Here we present the case for a more rigorous and detailed representation of flow resistance in hydrological models (see *Smith et al.* [2007] for a previous discussion), as flow routing velocities and travel times interact with infiltration and rainstorm structure to determine hillslope and catchment outflow. The spatial distribution of infiltration rates is not examined in detail as it is the focus of numerous other investigations [e.g., *Morin and Benyamini*, 1977; *Berndtsson and Larson*, 1987].

[10] The aim of this paper is to develop this conceptual model of semiarid hillslope hydrology through field observations, offering a quantitative perspective of dynamic connectivity. In doing so, we address the following research questions.

[11] 1. How does the temporal structure of rainfall events influence the formation of connected flow paths in semiarid areas?

[12] 2. Can controls on the spatial and temporal variability of flow resistance be identified?

[13] 3. How can results from plot-scale runoff experiments be upscaled to represent connectivity development over semiarid hillslopes?

[14] We present an integrated methodology to analyze the processes of connectivity development, encompassing rainfall-runoff analysis, mapping of hillslope microtopography, plot-scale flow experiments and the development of roughness-resistance relationships. A scheme through which these data sets (obtained at different scales) can be synthesized and incorporated into existing spatially distributed physically based hydrological models is presented.

## 2. Field Sites

[15] The Guadalentín River in southeast Spain is one of the most torrential rivers in the country. This investigation considers three hillslopes located in two semiarid catchments within that basin: the Rambla Nogalte catchment, which is on the border of the provinces of Murcia and Almeria, and the Rambla de Torrealvilla catchment, nearby in Murcia (Figure 1). This area of Spain is the driest part of the western Mediterranean; *Bracken et al.* [2008] report that the catchments receive approximately 300 mm of rain annually. These conditions provide a valuable exemplar of an environment that may become more widespread with projected future climate change [*Hooke and Mant*, 2000]. The three hillslopes examined represent the entire range of hydrological characteristics found on hillslopes within the catchments [*Bull et al.*, 2003], allowing this investigation to be as representative as possible. Each hill resembles a small headwater catchment, displaying a similar increase in slope angle with
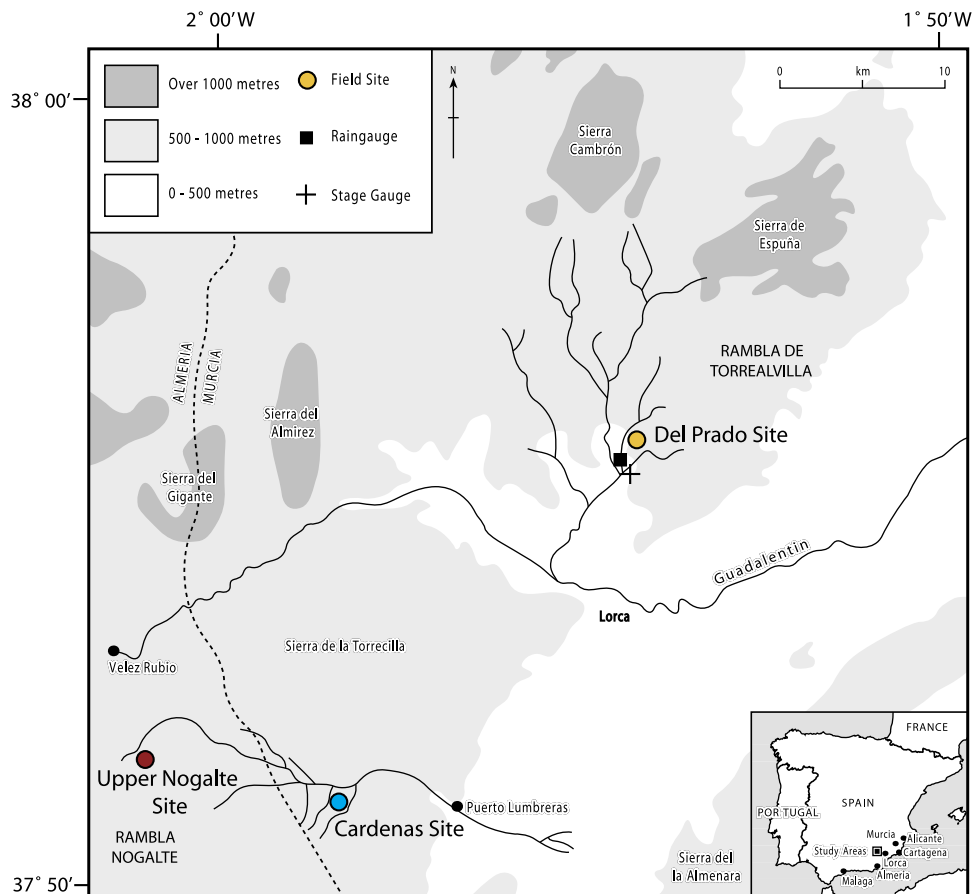
**Figure 1.** The study area in southeast Spain indicating the locations of field sites and rain and stage gauges (adapted from *Bracken and Kirkby* [2005, p. 185]).

distance downslope (2°–30°) before flattening out at the valley floor.

[16] The Upper Nogalte hillslope (2,787 m$^2$) is located in an area of red schist in the Nogalte catchment. This soil is low in clay minerals and high in quartz and feldspar, has a high infiltration capacity (>50 mm h$^{-1}$) and exhibits weak crust development. This area of the Nogalte catchment has a relatively high runoff threshold and is thought to be particularly unresponsive to rainfall [*Bracken and Kirkby*, 2005]. The Cardenas site (6,729 m$^2$) is situated in the Cardenas subcatchment. This area of blue schist is one of the key runoff-producing areas in the Nogalte catchment [*Bull et al.*, 2000, 2003]. The soil is high in clay minerals and platy fragments, susceptible to strong crust development, and considered to have a low runoff threshold with an infiltration capacity of <35 mm h$^{-1}$ [*Bracken and Kirkby*, 2005]. Finally, the Del Prado site (2,686 m$^2$) is situated on a bare area of marl in the Rambla de Torrealvilla, which is also suspected of producing large amounts of runoff. *Bull et al.* [2000] suggest that runoff thresholds are much lower on the marls of the Torrealvilla than on the schists of the Nogalte (infiltration capacity of <10 mm h$^{-1}$). The surface is composed mainly of fines, with evidence of both a structural crust and a lichen crust, and is mostly devoid of vegetation (with occasional grasses and thyme bushes covering ~10% of the surface area). A Metrolog system with Druk pressure transducers measured flow stage downstream of the Del Prado hillslope (Figure 1). A Casella 0.2 mm tipping bucket rain gauge also measured rainfall at this location. Both monitoring devices have been recording runoff and rainfall for 10 years, although short some gaps in the record exist.

## 3. Methodology

### 3.1. Rainfall-Runoff Analysis

[17] The ability of standard rainstorm analyses and more novel metrics to represent flood generation at the small catchment scale was compared. A flow stage of 20 mm was selected as the minimum threshold value for a runoff event, as it is observed that this depth of flow is necessary for connected flow down the ephemeral channel. The rainfall record was divided into spells, defined as periods of rainfall without breaks greater than 12 h. This criterion was selected to allow sufficient time for flow discontinuities to develop and the soil to dry out (see *Bracken et al.* [2008] for a full discussion). A data set of 24 runoff events so defined could be linked to rainstorms recorded at the adjacent rain gauge, representing an update of the data set previously presented by *Bracken et al.* [2008]. The largest runoff events were recorded in June 1997 and October 2000, although other large events are known to have occurred in this period (e.g., September 1997 [*Bull et al.*, 2000]) but were during gaps in the record available for this analysis (when monitoring equipment was damaged).

### 3.2. Overland Flow Measurement

[18] The objective of this component is to determine the controls on flow resistance using a new high-resolution methodology of measuring shallow flows over complex, partially inundated bare soil surfaces developed for this investigation. Overland flow was simulated from a constant discharge trough located at the upslope boundary of 15 plots (~2 m wide and 3 m in length) on natural, undisturbed, bare soil surfaces. Plots were distributed 5 per hillslope, systematically reflecting downslope transitions in micro-topography (section 3.3). The duration of each experiment was between 60 and 90 s. The supply trough was 0.81 m wide and provided a discharge of $0.52 \ l \ s^{-1} \ m^{-1}$ width (commensurate with flow depths observed on these hillslopes during intense storm events between July 2002 and August 2007). Once the initial flow front had advanced over the plot surface, three pulses of dye were added to the trough and each dye front was then tracked over the plot in the same manner. Up to three runoff experiments were undertaken at each plot: two on dry soils and one after a "wetting-up" rainfall event (of an insufficient magnitude to produce runoff, with just 13 mm of rain falling over 24 h). For logistical reasons, all three experimental runs could not be conducted at every plot. The measured velocity was not corrected for mean velocity due to the uncertainty surrounding the selection of such a velocity correction factor $\alpha$ [*Planchon et al.*, 2005] and because the main objective of this study is to examine *controls* on resistance and not the absolute value. Similarly, rainfall was not simulated in this study; consequently the resultant resistance values may be an order of magnitude smaller than that experienced by natural rain-induced flows [*Parsons et al.*, 1994].

[19] Sequences of overhead images of the advancing flow and dye pulses were taken at 1 s intervals from a camera boom. These images were later georeferenced over a 2 mm resolution digital elevation model (DEM) obtained from a Trimble GS200 terrestrial laser scanner. Each plot was scanned from multiple directions from a range of 3 m to limit occlusion effects. The scans were later merged in the Realworks software package. The registration operation was automated by surveying a minimum of five control targets for each scan. Reported registration errors were consistently below 2 mm. The achievable measurement precision was the main limitation to this study. An experiment was designed to reproduce the field methodology used here and establish the achievable precision by scanning calibrated roughness elements of a known size. The results suggested that a precision of at 1–2 mm is achievable, though roughness heights of as little as 0.3 mm could be detected [*Smith*, 2009]. This methodology is described in detail by *Smith et al.* [2010].

[20] Images taken at a known time interval georeferenced over a DEM provide sufficient information from which estimates of the hydraulic variables of overland flows can be extracted. At each time step the observed wet or dyed area was digitized (excluding any protruding dry areas within the wetted area) thus producing a sequence of outlines. Each sequence of advancing wet or dyed areas was divided into distinct flows demonstrating a similar advance of water between time steps (or "flow threads," similar to the "multiple partial sections" of *Abrahams et al.* [1986]). The flow within each thread is assumed to be uniform within each time step. The rationale behind dividing the flow in this way is to reduce

the error introduced by this assumption of uniformity [see *Smith et al.*, 2007].

[21] Measurements began after the flow had traveled at least 0.5 m from the supply trough (and the observed initial increase in velocity had steadied). Flow width $w$ was measured directly from the images. Velocity $V$ was calculated from the time interval and the maximum distance between a point on a flow outline and the nearest point of the previous wetted extent (and is thus an estimate of maximum velocity). The water surface of each flow thread was reconstructed using the flow extent and the underlying DEM. An algorithm was developed to estimate the water surface at each point on a cross section perpendicular to the flow direction. This algorithm is described by *Smith et al.* [2010] and was used to calculate water depth $d$ at each point of the 2 mm resolution DEM. These depth estimations are well correlated with point measures made in the field ($r = 0.834$, $P < 0.0001$); a linear regression between the two yields a coefficient of 1.017, suggesting a strong degree of concordance between the two methods of depth measurement. The concordance correlation, which measures agreement of variables rather than linearity of relationship is 0.820, only a little below the Pearson correlation [*Lin*, 1989, 2000; *Cox*, 2006]. The DEM calculation has the tendency to underestimate shallow depths slightly and overestimate larger ones.

[22] Width $w$, median depth $d$ and velocity $V$ were estimated for each thread at each time step. Cascades of such DEMs for a sequence of time steps allow flow resistance to be calculated using a modified version of Darcy-Weisbach's $f$. Following the original formulation of $f$, the measured energy gradient $S_f$ replaced soil surface slope as this incorporates acceleration or deceleration experienced by the flow between time steps. Second, the "volumetric hydraulic radius" $R_v$ (the ratio of the water volume to the bed surface area [*Smart et al.*, 2002]) replaced the depth or hydraulic radius term. This represents a more practical measure for overland flows, avoiding the problem of defining a datum from which to measure flow depth. Thus, given $g$ as the acceleration due to gravity, flow resistance $f$ was calculated as the dimensionless measure

$$f = \frac{8gR_vS_f}{V^2}. \tag{1}$$

Surface roughness measures were calculated for each flow thread at each time step. For complex surfaces this cannot be described by a finite number of parameters; thus a variety of measures were calculated. These include the roughness height, standard deviation of elevations, tortuosity measures (i.e., the ratio between measured area (or length) and that of the equivalent plane (or straight line)), density of pits, protruding frontal area measurements (surface area protruding directly into the flow), mean elevation difference between neighboring points and a nearest neighbor measure (minimum elevation difference between neighboring points). These roughness measures were calculated both over three dimensional surfaces and on transects divided into perpendicular components (both down and cross slope). The resulting data set was used to develop a suite of empirical equations relating $f$ to measures of surface roughness.

[23] Maximum depressional storage of each plot was calculated using the PCRaster GIS software [*Van Deursen and Wesseling*, 1992]. Point measurements of hydraulic

**Table 1.** Criteria Used to Identify Morphological Runoff Zones (MRZs) in the Field[a]

| MRZ | Types of Evidence Noted in the Field |
|---|---|
| 1 | surface crusting and armoring, splash pedestals, small areas of wash deposits |
| 2 | depositional steps ($<10$ cm$^2$) (often behind vegetation), larger areas of wash deposits ($<50$ cm$^2$) |
| 3 | some concentrated flow, erosional steps/small headcuts |
| 4 | concentrated rills ($\sim 0.1$ m$^2$) |
| 5 | gullies ($>1$ m deep) with own side slopes |

[a]Source: *Bracken and Kirkby* [2005, p. 187].

conductivity were taken over each of the hillslopes using a minidisk tension infiltrometer, an acrylic tube with a semi-permeable plastic disk as a base. A small tube installed just above the disk regulates the suction (2 cm). It takes a reading over an area 20 mm in diameter, and so can assess the variability of infiltration rates at a scale appropriate for this investigation. The minidisk has been shown to produce results consistent with measures of field infiltration rates from rainfall simulation [*Zhang*, 1997; *Li et al.*, 2005]. Ten measurements were made on each plot, distributed between roughness elements.

### 3.3. Morphological Runoff Zones

[24] Extrapolating plot-based studies to larger areas is problematic in the face of heterogeneous landscape properties. Investigations of hydrological connectivity must select a sampling strategy that provides a suitable description of the heterogeneities that have a profound influence on runoff response at the hillslope scale [*Ali and Roy*, 2009]. This study attempts to upscale results from runoff plots to the hillslope scale. The primary focus is an examination of the effect of soil surface morphology on flow resistance and velocity; thus runoff plots were distributed according to areas demonstrating similar microtopography as observed in the field. While it is recognized that the location and configuration of vegetative elements on such hillslopes is an important control of connectivity development [e.g., *Cammeraat*, 2004], this study is presently limited to bare soil surfaces.

[25] Moving downslope from the drainage divide, the microtopography of soil surfaces displays systematic shifts as the upslope contributing area increases and advective runoff incises the soil surface [*Horton*, 1945; *Smith and Bretherton*, 1972]. *Bracken and Kirkby* [2005] mapped morphological evidence of runoff intensity on semiarid hillslopes and classified the surfaces into five morphological runoff zones (MRZs) based on observed surface features outlined in Table 1. This qualitative classification was used to distribute plot locations systematically over each hillslope (one plot per MRZ), ensuring that emergent properties at the hillslope scale are included in this analysis.

[26] The extent of each MRZ (and any ploughed areas) was mapped using a handheld GPS device (GS20). The mapped distribution of MRZs was then draped over a 50 mm resolution Digital Elevation Model (DEM) of each hillslope obtained using the Trimble GS200 laser scanner. The survey method employed at the hillslope scale was similar to that employed at the runoff plots over distances an order of

magnitude larger. There was greater variation around the target resolution of 20 mm due to the hillslope form. However, between 3 and 5 hillslope-scale scans were merged to reduce these effects and avoid occlusion issues presented by almond trees. Such large obstacles were manually removed from the resultant point clouds. Several areas of the hillslopes were covered with low-lying shrubs so that a thick density of foliage was present near the soil surface. Being so close to the soil surface, they are likely to affect surface processes and thus remained in the hillslope scans. This may influence upslope contributing area calculations which were made using a deterministic eight node flow routing algorithm (chosen as it performs reasonably well over the relatively rough hillslope surfaces and allows individual flow pathways to be tracked).

[27] *Kirkby et al.* [2005] observed that morphological runoff zones are consistently related to the overland flow length-slope product within the same lithology and land use and that differences in the length-slope product reflect differences in runoff response. The length-slope product can be used to identify a threshold for erosion for each MRZ identified in the field. Integrating field maps with hillslope DEMs allows the identification of length-slope thresholds for the development of surface morphological features and thus provides an index-based methodology of upscaling results obtained from runoff plots.

## 4. Results

### 4.1. Rainfall Characteristics and Runoff Response

[28] Rainfall characteristics are key drivers of flood generation in all hydrological models, yet the connectivity framework places greater importance on the fine structure of such rainfall events. Figures 2 and 3 show the relationships between summary rainfall characteristics and runoff generation for the Prado tributary of the Rambla de Torrealvilla into which the Del Prado hillslope drains via a system of gullies. Correlations between rainfall characteristics and flow stage measured at the Prado are given in Table 2. For comparison, with this sample size of 24 and normality and independence assumptions satisfied, a correlation of 0.34 would be significant at the 1% level.

[29] Total storm rainfall is well correlated with runoff generation; the largest flood peaks were produced from the largest total rainfalls. Despite some scatter around intermediate events, the relationship is significant at the 1% level. Both mean and maximum storm intensity are also significant at this level with a slightly stronger relationship evident between runoff and maximum intensity. Storm duration did not show a direct relationship with peak stage (although this will be affected by the selection of a 12 h rain-free interval between spells). However, Figure 2 shows that two outliers are found where two of the largest runoff events were generated from relatively short-lived storms (of June 1997 and May 2004). These outliers were not found where rainfall intensity or depth measures are incorporated into the analysis.

[30] Previous research has suggested that hillslope-scale flood generation is influenced by the relationship between infiltration rate and storm intensity [e.g., *Reaney et al.*, 2007]. Variations in storm intensity, direction and velocity have been observed to generate distinct hydrological and erosional responses in laboratory experiments [*de Lima et al.*, 2003].
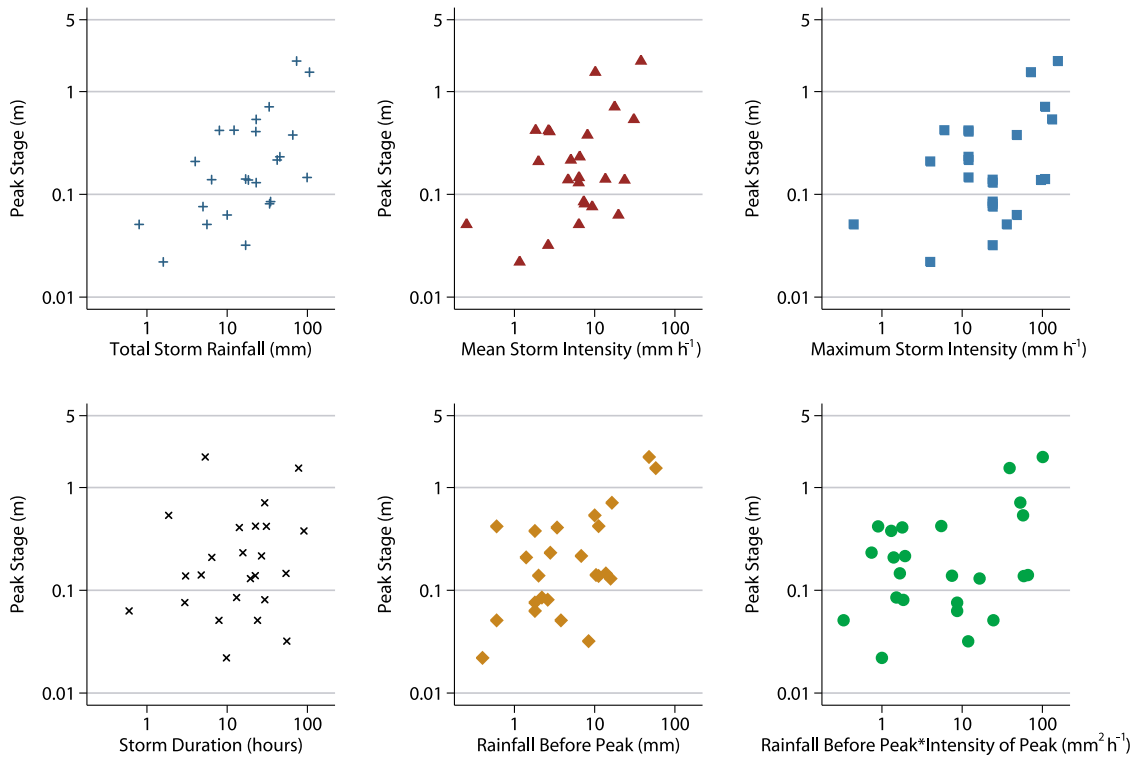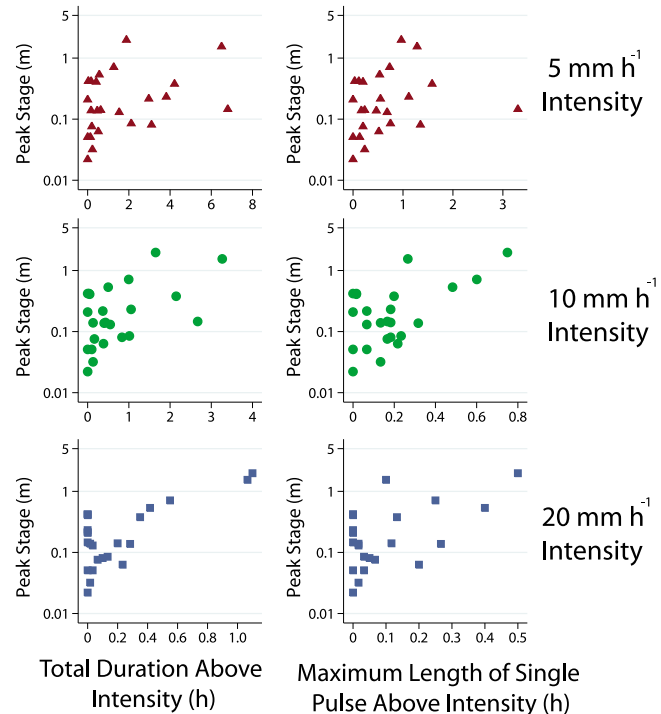
**Figure 2.** Relationships between flood generation and storm characteristics at the subcatchment scale for the Prado tributary of the Rambla de Torrealvilla.

Where infiltration rate declines during the course of a rainstorm, the location of a high-intensity burst or pulse of rain within that storm event will affect flood peaks. This can be assessed quantitatively as the depth of rainfall that has fallen before the intensity peak is reached. Figure 2 shows the strong relationship between this measure and flood stage and demonstrates that adding an appreciation of the value of the peak intensity does not improve the relationship (the correlation coefficient drops substantially, although the relationship remains significant at the 1% level).

[31] Figure 3 further examines the influence of intense pulses of rainfall on runoff generation. For three thresholds (5, 10 and 20 mm h$^{-1}$), the relationships are shown between peak stage and total time within each storm experiencing rainfall above this threshold and also the maximum continuous duration of a single pulse above the intensity threshold. Both total duration above 5 mm h$^{-1}$ and maximum pulse duration above 5 mm h$^{-1}$ were uncorrelated with peak stage, suggesting that the Prado catchment has a higher runoff threshold. Indeed, at 10 and 20 mm h$^{-1}$ the relationships are significant at the 1% level. The total duration above 20 mm h$^{-1}$ was well correlated with peak stage ($r = 0.90$); this relationship appears to be especially strong for the largest runoff events.

[32] The maximum duration of a continuous pulse was better correlated with flood generation for the 10 mm h$^{-1}$ threshold. This measure is complicated by the number of pulses experienced during the course of a storm event (a pulse is terminated even if the rain falls below the threshold for just one minute). This is evident in Figure 3 where outliers at the 10 and 20 mm h$^{-1}$ thresholds experienced a short continuous pulse duration but a large number of pulses during the



**Figure 3.** Relationships between flood generation and storm characteristics at the subcatchment scale for three rainfall intensity thresholds for the Prado tributary of the Rambla de Torrealvilla.

**Table 2.** Correlations Between Rainfall Characteristics and Peak Stage at the Prado Tributary[a]

| $n = 24$ | Peak Stage |
|---|---|
| Total storm rainfall | 0.61 |
| Mean storm intensity | 0.57 |
| Maximum storm intensity | 0.62 |
| Storm duration | 0.20[Δ] |
| Rainfall before peak intensity | 0.89 |
| Rain before peak × intensity of peak | 0.64 |
| Duration above 5 mm h$^{-1}$ | 0.33[Δ] |
| Maximum pulse duration, 5 mm h$^{-1}$ | 0.20[Δ] |
| Duration above 10 mm h$^{-1}$ | 0.56 |
| Maximum pulse duration, 10 mm h$^{-1}$ | 0.66 |
| Duration above 20 mm h$^{-1}$ | 0.90 |
| Maximum pulse duration, 20 mm h$^{-1}$ | 0.61 |

[a]All correlations are significant at the 1% level unless otherwise indicated with a delta (where relationships are not significant).

rainstorms. The three large flood events with lower pulse duration at the 20 mm h$^{-1}$ intensity were much longer storms (>24 h, frontal-driven events) than the four below them (0.6–5.3 h, most probably convective-driven events).

Figure 3 shows that the total time above the 20 mm h$^{-1}$ intensity threshold is more important than the length of individual pulses.

### 4.2. Thresholds of MRZs: Upscaling Framework

[33] Figure 4a displays a plan view of each hillslope in this study with the field maps of morphological runoff zones (MRZs) overlaid. These maps are of insufficient resolution to separate flow concentrations from surrounding interrill areas; thus they represent a first approximation used to provide an estimate of MRZ thresholds at each hillslope. At the lower boundaries of each MRZ, the product of the slope and the square root of the upslope area was calculated (maintaining the same units as *Kirkby et al.* [2005]).

[34] A relatively consistent relationship between the slope and upslope area is observed at the lower boundaries of each MRZ (Figure 5). Beyond certain thresholds in the slope-area product, wash deposits (below the downslope limit of MRZ 1), flow concentrations (below MRZ 2), rills (below MRZ 3) and gullies (below MRZ 4) form. The Cardenas hillslope has the highest threshold for the downslope limit of
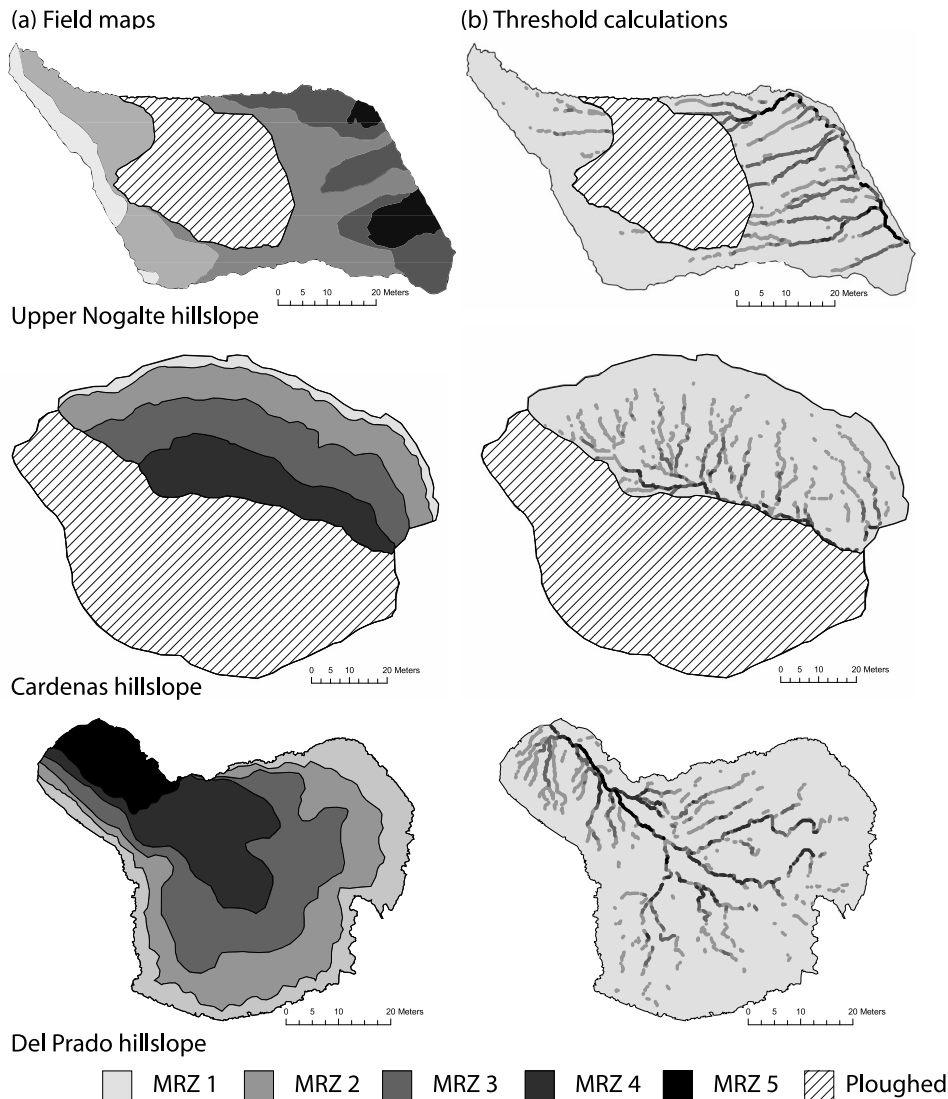


**Figure 4.** Distribution of morphological runoff zones on each hillslope: (a) field maps and (b) calculated distribution of flow paths over each threshold.
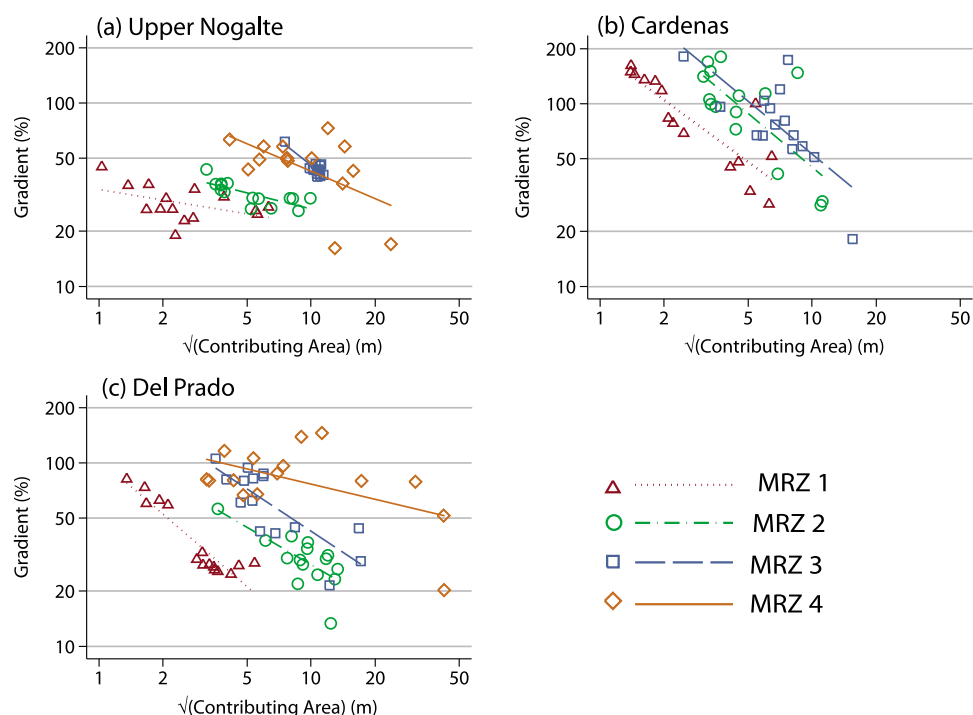
**Figure 5.** The relationship between the square root of the upslope area and gradient for different morphological runoff zones at each hillslope.

each MRZ. The gradient of these thresholds varies between each hillslope, reflecting differences in either soil erodibility or runoff response; a steeper threshold slope-area relationship in Figure 5 suggests that incision occurs at lower contributing areas (at any given slope angle). This indicates the dominance of the upslope area measure in determining the erosional threshold (possibly a consequence of high runoff response). The Cardenas hillslope shows the steepest threshold lines followed by the Del Prado and Upper Nogalte hillslopes. Shallower thresholds in Figure 5 indicate a greater influence of gradient in the onset of these features (possibly identifying more erodible soils). The MRZ 4 lower thresholds are generally shallower with a dominance of slope gradient determining the onset of gully erosion. The crossover between the downslope boundaries of MRZ 3 and MRZ 4 at the Upper Nogalte hillslope represents the absence of a lower MRZ 4 boundary over parts of the hillslope (Figure 4a).

[35] Thresholds for each MRZ were estimated for each hillslope from the DEM, calculated as the product of the maximum of the square root of the upslope area found in each MRZ and the mean slope angle of the mapped area. Mean slope was used to limit the effect of localized steep slopes on threshold calculations. This measure provided an approximate threshold for each MRZ which can be derived from the DEM alone. These thresholds were then applied to each hillslope DEM to give a prediction of the locations of each MRZ (Figure 4b). This avoids the problematic lumping of areas of low contributing area with rills and flow concentrations.

[36] The Cardenas hillslope demonstrates the largest value of the slope-area product before each level of morphological features is observed. This area has been shown to have a relatively low runoff threshold [*Bull et al.*, 2000] suggesting that the soils of this hillslope are the least erodible (see also

Figure 5). The Del Prado slope requires a much lower slope-area product for erosion to initiate. The predicted threshold values of the Upper Nogalte hillslope are difficult to interpret because the natural grading of the morphological runoff zones is interrupted by the presence of a ploughed band (the base of the MRZ 2 plot is artificial). Previous research [e.g., *Bull et al.*, 2003] indicated that the red schist of the Upper Nogalte hillslope has the lowest runoff response. It was expected that this hillslope should have the highest threshold of the three hillslopes. While this was not the case, the shallow slope-area relationship in Figure 5 suggests that slope angle is a more influential factor of erosion thresholds than upslope area (and runoff response).

[37] The maps of morphological runoff zone locations calculated from the erosion thresholds in Figure 4b are very different from the field sketches. The procedure outlined here provides an index-based method of upscaling plot measurements of flow resistance to the hillslope while preserving hydrological connectivity and limiting the designated MRZ 2–5 areas to just those specific flow lines where concentrated flows occur.

## 4.3. Overland Flow Measurements

[38] Hydrological connectivity is a function of both runoff production and transfer; at the hillslope scale this is strongly associated with flow path development and influenced by travel times both over interrill surfaces and through flow concentrations [e.g., *Kuhn and Yair*, 2004; *Reaney*, 2008]. The distinct surface morphologies as classified by the morphological runoff zone framework present a range of flow conditions and velocities (defined here as the downslope vector of the scalar quantity speed), primarily due to their ability to concentrate runoff into more efficient flow pathways. This is evident in Figure 6 where the differential ability of each
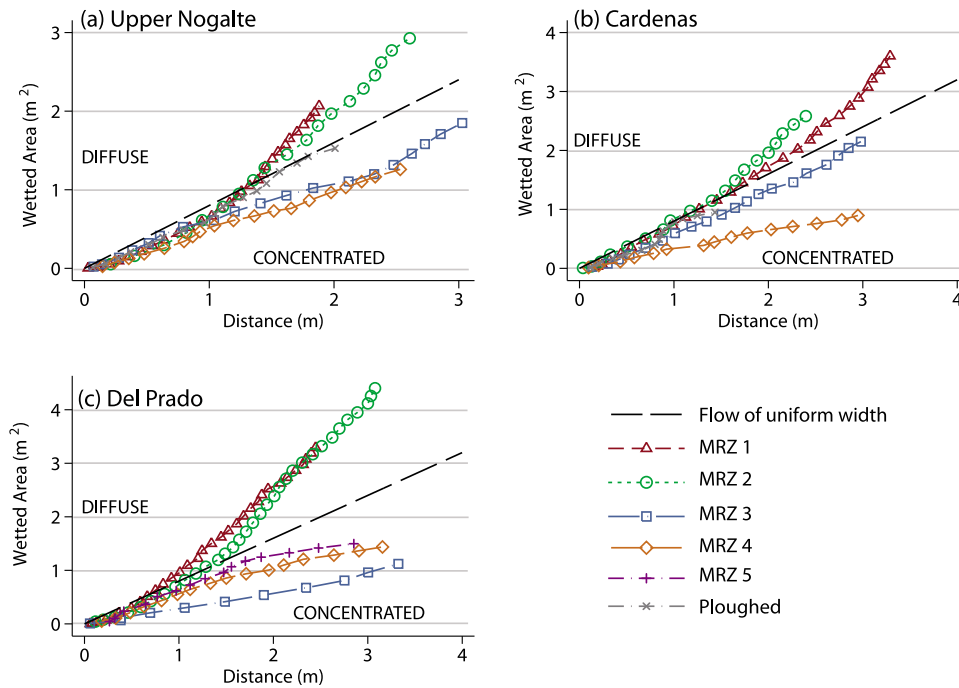
**Figure 6.** Increase of wetted area with distance traveled for each plot and hillslope.

MRZ to concentrate flow during simulation experiments can be clearly observed. At each hillslope, the upslope locations (MRZs 1 and 2) produce diffuse flow. The degree of flow concentration increases with distance downslope. The Del Prado hillslope provides an exception to this pattern where flow is most concentrated in the narrow flow concentrations and becomes less confined as the rills and gullies develop gradually wider beds further downslope. This may reflect the greater amount of runoff thought to be produced at this site, carving more developed erosional features. Indeed, the degree of flow concentration observed in Figure 6 is a function of the imposed discharge in the flow experiments.

[39] Flow velocity was observed to increase with the degree of concentration, although this effect was most pronounced at the MRZ 3 and 4 plots. At each degree of concentration the Del Prado hillslope recorded the highest velocities and Upper Nogalte the lowest. Figure 7 presents the median velocities recorded within each plot. The pattern of velocities between MRZs was similar for each hillslope, suggesting that the categorization of MRZs is appropriate at the hillslope scale. Velocity measurements varied substantially within each plot, especially within flow concentrations and rills where faster flow was recorded. The hydraulic behavior of flow through rill networks will greatly affect the hydrological response of a hillslope as much of the generated runoff will be routed through such flow concentrations.

[40] Figure 7 compares median velocities at each plot under different soil moisture conditions. Recent studies (and the results in Figure 2) show that antecedent soil moisture is a key factor for runoff and flood generation in semiarid environments [e.g., *van de Giesen et al.*, 2000; *Aryal et al.*, 2003; *Yair and Raz-Yassif*, 2004; *Reaney et al.*, 2007]. Yet Figure 7 shows no obvious or consistent differences between flow velocity during wet and dry runs. At the Cardenas hillslope velocity is slightly greater during the wet

runs; this effect is more prominent at the downslope locations. However, at the Upper Nogalte and Del Prado hillslopes, runoff transfer may be faster over dry surfaces. The three experimental runs at each MRZ of the Del Prado hillslope show no consistent differences. The effect of antecedent conditions observed in the rainfall record is thus limited to runoff generation and has a negligible influence on runoff transfer.

[41] Overland flow velocities interact with both the geometry and integration of the drainage pattern [e.g., *Kuhn and Yair*, 2004] and the distribution of flow path lengths [e.g., *Kirkby et al.*, 2005] to influence hillslope outflow. Figure 8 demonstrates the effect of scaling-up median flow velocities to the hillslope applying the values of Figure 7 to the calculated distribution of MRZs at the Del Prado hillslope. The result is a basic Instantaneous Unit Hydrograph [e.g., *Sherman*, 1932; *Nash*, 1957; *Rodríguez-Iturbe and Valdès*, 1979] directly informed by field measurements of flow velocity and distributed by morphological runoff zone (as calculated in Figure 4b).

[42] Two distinct peaks in the travel time distribution can be observed (Figure 8b). The smaller, sharper first peak arrives after about 3 min and was observed for all three simulations. This peak is a product of the efficient routing of runoff through the rill and gully system at the foot of the hillslope (Figure 4b). This efficient flow routing can be seen from the 1 min isochrones of Figure 8a. The larger second peak arrives after 6 min; comparison of Figure 8b with the 1 min isochrones suggests that reflects the hydrological connection of the large area at the top of the hillslope to the outlet. Differences in the travel time distributions are most defined at the Del Prado hillslope, although only small differences can be detected. Both dry soil runs have a flatter peak travel time distribution; the wet soil experiment has the highest and most defined peak. Where transmission losses
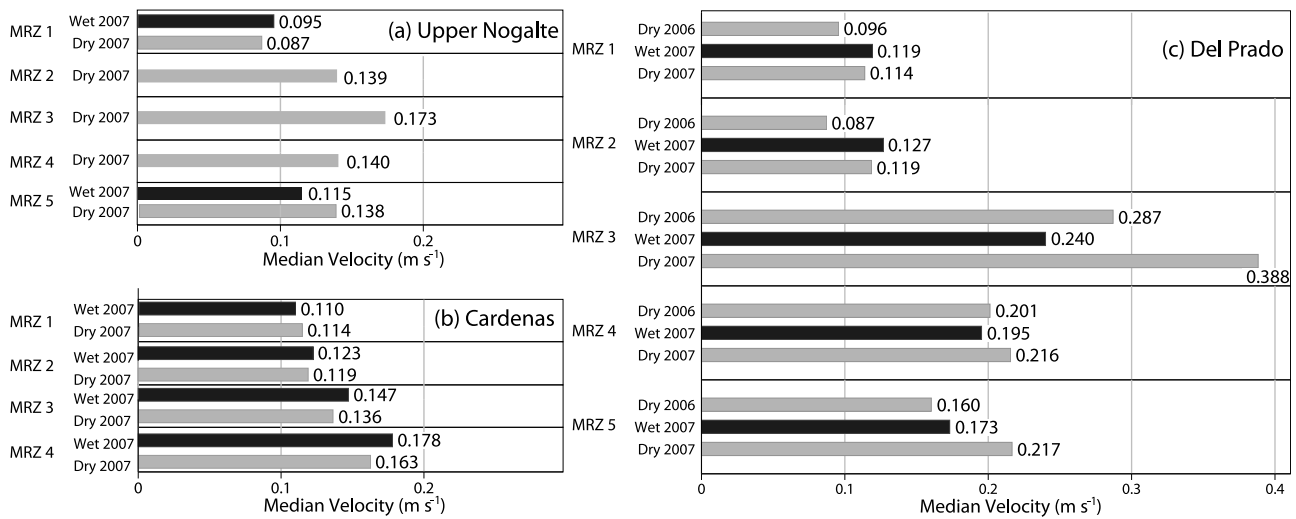
**Figure 7.** Median flow velocities under different soil moisture conditions.

are considerable (e.g., semiarid hillslopes) such superimposition of runoff volumes increases the likelihood of water reaching the channel and is thus a key component of hydrological connectivity. The travel time of this wet soil run is intermediate between the two dry runs. It appears that the overall morphology of the hillslope dominates travel time distributions with little effect of antecedent soil moisture on runoff transfer. This basic analysis demonstrates the importance of including the interaction between overland flow velocity and hillslope morphology in any attempt to quantify hydrological connectivity.

### 4.4. Spatial Variation of Flow Resistance

[43] The approach demonstrated in Figure 8 applies the observed median flow velocities (at a single imposed discharge) to estimate the effect of hillslope morphology on hillslope travel times, thus ignoring the variability of flow velocity observed at each MRZ. A better approach to routing velocities is to predict $V$ using equation (1) and integrate over the path length of the flow (see section 6). This requires an estimation of flow resistance over the hillslope surface. Figure 9 shows that measured flow resistance is variable even over a plot surface. The Cardenas hillslope shows the greatest resistance and most pronounced increase in $f$ downslope; this pattern is less obvious at the other two hillslopes. The Del Prado plots show the lowest resistance and widest range of $f$ values. Very low $f$ values were recorded on shallow slopes and are subject to error where the surface roughness dominates the overall topography (resulting in slopes that were close to zero). The length scale used to measure the
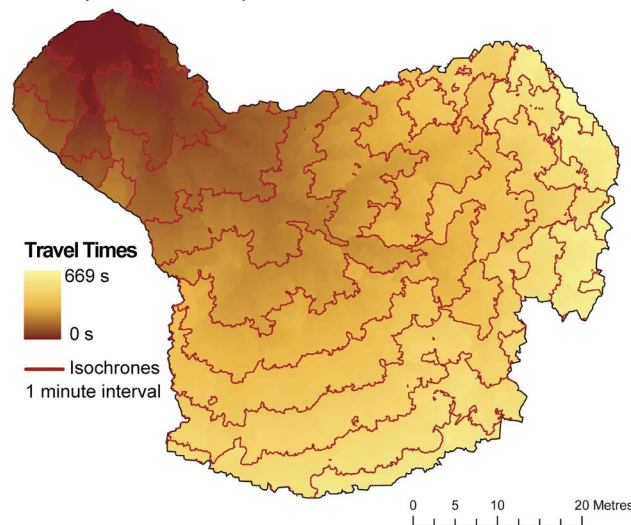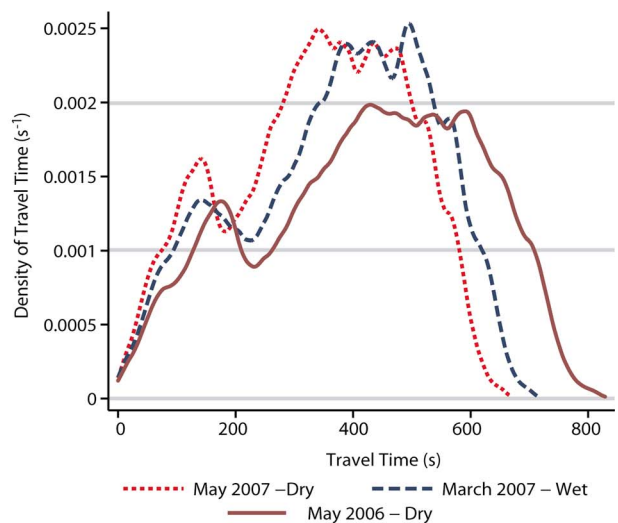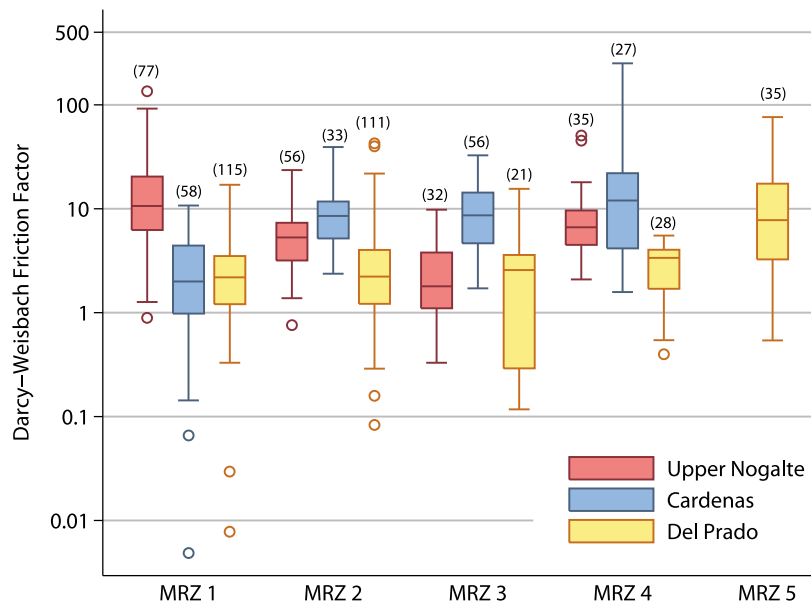


**Figure 8.** (a) Travel times calculated for the Del Prado hillslope using data from the May 2007 experiments and (b) kernel density estimate of the probability density function of travel times (using the Epanechnikov kernel with a half width of 10 s [Cox, 2007]).

**Figure 9.** Variation of the Darcy-Weisbach friction factor between each plot and hillslope. Morphological runoff zones (MRZs) relate to hillslope position (moving downslope 1–5) and are described in Table 1. Only the Del Prado hillslope contained evidence of gully erosion (MRZ 5). Boxes show upper quartiles, medians, and lower quartiles; whiskers extend to cover all points within 1.5 times the interquartile range of the quartiles; and other points are shown separately. Numbers in parentheses represent the number of observations for each plot.

energy slope was determined by the 1 s interval of flow measurements and thus varies over each hillslope. Increasing this length scale would reduce the range of resistances recorded. This approach to defining a length scale was chosen as it is well suited to hillslope hydrological models operating at a time step of 1 s. This establishes a necessary working distinction between roughness (sub-time step scale) and topography.

### 4.5. Temporal Variation of Flow Resistance

[44] Thus far we have operated under the assumption that flow resistance is constant. Yet, relationships between flow resistance and surface roughness measures demonstrate the dependency of resistance on flow depth (incorporating measures of relative submergence, e.g., the inundation ratio of *Lawrence* [1997]). The development of empirical resistance equations from a number of surface roughness measures is described in detail by *Smith et al.* [2010]. A summary is presented in Table 3. The entire soil surface is not always inundated by shallow overland flows. As water surface level increases, the complex microtopography of natural soil surfaces introduces a nonlinear dependency on flow depth. The modeled depth dependency at each MRZ is summarized using a natural spline (a piecewise smooth function [*Harrell*, 2001]) while the observed distribution of non-depth-dependent roughness measures (e.g., protruding frontal area, standard deviation of elevations) is used to obtain a range of resistance predictions. Figure 10 presents summary percentiles of the predicted resistance distribution for the Del Prado hillslope (used to generate the flow resistance patterns of Figure 12). These predictions are validated with independent observations obtained from separate experiments imposing a variable discharge on soil surfaces on the same hillslope (made at two locations for each MRZ) and show

a good overall agreement. Given the variability observed in Figure 9, these two locations will lie within a larger spread of data points expected from a larger validation data set (the minimum extent of this is summarized with an ellipsoid in Figure 10).

[45] Once a hydrological connection has been initiated, the flow resistance was observed to drop by over 80%. A comparison of flow resistance measures from the first water wave and subsequent dye flow measurements demonstrates this (Figure 11a). At the Del Prado hillslope, the roughness-resistance equations used to generate the curves of Figure 10 overpredict this resistance (Figure 11b). Unsaturated hydraulic conductivity and maximum depression storage offer potential explanations for the drop in resistance (Figures 11c and 11d), yet no consistent patterns emerge. This agrees with the observation that antecedent soil moisture conditions have little effect on overland flow routing velocity (Figure 7).

### 5. Discussion

[46] Here we present the first steps toward a quantification of hydrological connectivity for semiarid hillslopes that encompasses both structural and dynamic components. Given the combined importance of spatial patterns of both runoff generation and transfer, connectivity metrics must reflect this interaction. Representation of the spatial and temporal variability of flow resistance $f$ must be integral. We offer a preliminary overview of this process, outlining relevant hydrological properties, basic initial results, and a research strategy for achieving this goal.

[47] Analysis of rainfall characteristics at the Prado tributary suggests that conventional rainfall summaries (e.g., total duration, mean intensity) give an incomplete picture of the processes relevant to connectivity development. The

**Table 3.** Summary of Roughness-Resistance Relationships Developed[a]

| Plot | Roughness Equation | Predictors | | | $R^2$ |
|---|---|---|---|---|---|
| GENERAL | $f = \dfrac{e^{4.9S+1.2\Lambda-1.34F_P}}{4(\sigma_Z P_{dxc})^{0.77}}$ | $S$ | $+$ | slope | 0.59 |
| | | $\Lambda$ | $+$ | inundation ratio | |
| | | $F_P$ | $-$ | frontal area per m² | |
| | | $P_{dxc}$ | $-$ | perpendicular pit density | |
| MRZ 1 | $f = e^{4S+2\Lambda-1.8F_P-1.5(\sigma_Z P_{dxc})}$ | $\sigma_Z$ | $-$ | elevation SD | 0.56 |
| | | $S$ | $+$ | slope | |
| | | $\Lambda$ | $+$ | inundation ratio | |
| | | $F_P$ | $-$ | frontal area per m² | |
| | | $P_{dxc}$ | $-$ | perpendicular pit density | |
| MRZ 2 | $f = \dfrac{e^{6S+1.4\Lambda-190d_{50}}}{7(\sigma_Z P_{dxc})^{0.63}}$ | $\sigma_Z$ | $-$ | elevation SD | 0.73 |
| | | $S$ | $+$ | slope | |
| | | $\Lambda$ | $+$ | inundation ratio | |
| | | $F_P$ | $-$ | frontal area per m² | |
| | | $P_{dxc}$ | $-$ | pit density (perp) | |
| MRZ 3 | $f = \dfrac{e^{5.7S}\Lambda^{0.5}}{7(\sigma_Z P_{dxc})^{1.36}}$ | $\sigma_Z$ | $-$ | elevation SD | 0.78 |
| | | $S$ | $+$ | slope | |
| | | $\Lambda$ | $+$ | inundation ratio | |
| | | $F_P$ | $-$ | frontal area per m² | |
| | | $P_{dxc}$ | $-$ | perpendicular pit density | |
| MRZ 4 | $f = \dfrac{e^{6.2S}}{4D_{sk}^{0.89}(\sigma_Z P_{dd})^{0.95}}$ | $\sigma_Z$ | $-$ | elevation SD | 0.73 |
| | | $S$ | $+$ | slope | |
| | | $\Lambda$ | $+$ | inundation ratio | |
| | | $F_P$ | $-$ | frontal area (per m²) | |
| | | $P_{dxc}$ | $-$ | perpendicular pit density | |
| MRZ 5 | $f = \dfrac{e^{6S+3.6\Lambda}}{23(\sigma_Z P_{dxc})^{0.6}}$ | $\sigma_Z$ | $-$ | elevation SD | 0.72 |
| | | $S$ | $+$ | slope | |
| | | $\Lambda$ | $+$ | inundation ratio | |
| | | $F_P$ | $-$ | frontal area per m² | |
| | | $P_{dxc}$ | $-$ | perpendicular pit density | |
| | | $\sigma_Z$ | $-$ | elevation SD | |

[a]Plus and minus indicate the direction of the relationship with resistance (measured by $f$). SD means standard deviation. For a more complete explanation, see *Smith et al.* [2010].

total duration above an intensity threshold of 20 mm h$^{-1}$ provides a simpler and equally effective measure of relevant rainfall characteristics than identifying individual bursts of high-intensity rainfall. The importance of the length of such pulses remains unclear; however, the location of high-intensity rainfall within a rainfall time series has an important effect on flood generation. A comparison of rainfall characteristics with flood magnitudes at the Prado tributary shows that measures incorporating an appreciation of the ratio between rainfall intensity and infiltration rate and the duration for which this ratio is above a certain threshold best represent the processes responsible for flood generation.

[48] *Bracken and Croke* [2007] note that dynamic connectivity includes the effect of soil moisture conditions and rainfall inputs on hydrological response, but also the longer-term evolution of the landscape including feedbacks between runoff transfer and topographic form through erosion and deposition. This emergent interaction (also expressed as "patterns, processes and functions" [e.g., *Sivapalan*, 2005; *Schröder*, 2006; *McDonnell et al.*, 2007]) provides a coherent and reproducible pattern through which to engage in an analysis of hillslope hydrology, producing results of greater transferability and more general applicability than studies focused on small-scale heterogeneities [*McDonnell et al.*, 2007]. It is represented here as the observed and calculated distribution of morpho-logical runoff zones (though these emergent patterns could equally be classified in a number of different ways). This example of structural connectivity is the result of previous functional connectivity; a feedback which can be used to inform the examination of future flood generation by classifying flow resistance estimates by the observed structural units (Figure 10). This approach provides a scaling tool to represent contiguous areas of high and low resistance across a hillslope and is analogous to the classification of surfaces of similar hydrological response discussed earlier.

[49] The maps of morphological runoff zone locations calculated from the erosion thresholds in Figure 4b are very different from the field sketches. This provides an index-based method of identifying MRZs and limits the designated MRZ 2–5 areas to just those specific flow lines where concentrated flows occur. Although this reduces their spatial coverage, these incisional flow paths remain crucial for hydrological connectivity and flood generation, as much of the hillslope runoff must be routed through them before reaching the outlet [e.g., *Croke and Mockler*, 2001]. The maps of Figure 4b provide a method of upscaling plot-based measurements to the hillslope scale, maintaining those heterogeneities that are crucial for modeling hydrological connectivity. For example, this approach was able to simulate discontinuities in the flow network, thus giving a more accurate interpretation of the location of flow concentrations than the mapped extents. At the Del Prado hillslope, a small discontinuity in the rill network was observed, most probably as a consequence of the gentle slope at a patch of the hillslope. As a result, rills become much less defined immediately upstream from their convergence into a gully (Figure 4b). Mapping such features in the field would be time consuming and relatively subjective. Through its dependence on slope angle, the erosion threshold applied to the hillslope DEM was able to reproduce this feature independently (Figure 4b). While such a discontinuity over a small area may seem inconsequential, even the smallest discontinuities in the flow network are of hydrological significance when viewed through the framework of hydrological connectivity [e.g., *Fitzjohn et al.*, 1998; *Cammeraat*, 2004]. Similar reversals of the normal downslope MRZ transitions are predicted at each of the hillslopes studied. Calculating MRZs in this way thus integrates the effect of high drainage density on steeper slopes [*Kirkby et al.*, 2005] and provides an appreciation of variability in the flow path downstream from each point.

[50] Classification of areas of similar flow features ignores the different infiltration rates observed across the hillslopes. Some patches may absorb more rainfall and therefore remain disconnected from the hillslope outlet, altering the effective contributing area [e.g., *van de Giesen et al.* 2000; *Yair and Kossovsky*, 2002]. However, it is the spatial configuration of runoff-producing areas and areas of high infiltration *alongside* areas of high and low flow resistance that is the key to understanding hillslope hydrological responses. The technique described in this paper provides a basic understanding of such spatial relationships. Assuming that the spatial variation of rainfall and soil erodibility is relatively unimportant at this scale, any disparities between the predicted extent of rill erosion (for example) and that observed in the field may be explained by the presence of an area with a high (or low) infiltration capacity relative to the hillslope average.
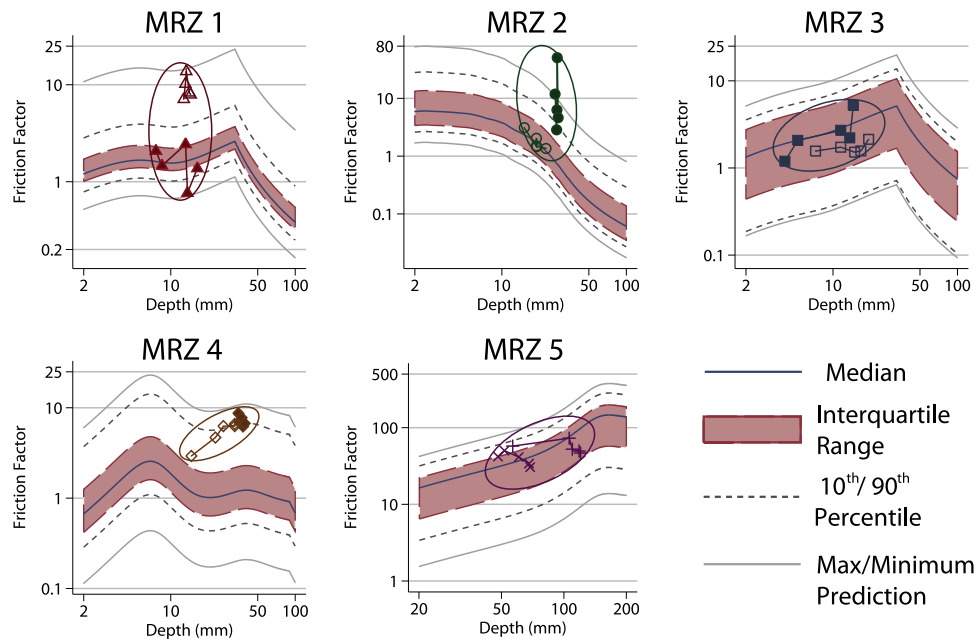
**Figure 10.** Summary percentiles of predicted flow resistance against median flow depth (mm) for the Del Prado hillslope using the regression equations developed separately for each MRZ (Table 3). Connected data points represent independent observations of flow resistance obtained from variable discharge experiments. Solid and open symbols distinguish each transect within an MRZ (represented by symbol shape). The minimum spread of the validation data set is indicated with an ellipsoid.

[51] Flow resistance can be estimated from measures of surface roughness. Given the range of observed flow resistance even at a single plot (Figure 9) such predictions should incorporate this variability. Various methods of representing flow resistance at the hillslope scale are available. Typically, flow resistance is represented as a single constant, lumping together entire hillslopes [e.g., *Morgan et al.*, 1998]. Several studies have observed that hydrological response is extremely sensitive to this resistance parameter, as higher friction factors increase run-on infiltration and decrease hydrological connectivity [e.g., *Wainwright and Parsons*, 2002]. The flow experiments conducted in this study revealed a large variability of flow resistance over small areas. This may be expected where flows are extremely shallow and the soil micro-topography is complex and heterogeneous. *Michaelides and Wainwright* [2002] found that increasing the spatial variability of resistance increased the variability of outflow. Adding an appreciation of this variability (from an estimate of the spatial continuity of such values [e.g., *Western et al.*, 1998]) produces an extremely patchy distribution of flow resistance. Alternatively, the calculated distribution of MRZs can be used to distribute values of *f* into structural units, thereby providing an appreciation of the connectivity of areas of high and low resistance. Given the observed variability of resistance even within areas of similar surface morphology, this would overestimate such structural connectivity; thus an appreciation of both spatial variability and classification is proposed here.

[52] The central argument of this paper is that flow resistance over semiarid hillslopes is both spatially variable and dependent on flow depth and should be represented as such in models of hillslope hydrology. The summary curves of Figure 10 were obtained from empirical equations predicting flow resistance from surface roughness measure-

ments. While the finer details of these predictions may be simply artifacts of these regression equations (which require further development), each equation demonstrated a depth dependency of flow resistance.

[53] Figure 11 also shows that flow resistance declines rapidly once a surface hydrological connection has been established, thus placing further emphasis on the temporal structure of rainfall intensities and duration of high-intensity rainfall. Differences between plots offer an opportunity for an examination of the factors responsible for the decreasing resistance with increased duration of a flow connection and increasing strength of delivery pathway (as would develop through a storm event once a hydrological connection is established [*Bracken and Croke*, 2007]). Several hypotheses can be identified to explain this shift. The decreased resistance may be due to one or more of the following: (1) decreased infiltration losses and associated suction forces, (2) filling of the depression store and induced turbulence, (3) reduced energy loss from three-dimensional flow vectors, (4) alteration of roughness measures between first wave and dye pulses, and (5) natural variability between measurements.

[54] Although infiltration losses and depression storage are not usually incorporated into flow resistance measures, in practice, the intermittent and complex nature of overland flows complicates attempts to maintain this distinction. The observed systematic and pronounced decrease in resistance suggest that hypothesis 5 alone is insufficient to explain the observed variability. Figures 11b–11d compare the overprediction with both unsaturated hydraulic conductivity and maximum depressional storage, yet no consistent patterns can be observed. The high degree of overprediction at the MRZ 5 plot may be explained by the filling of the depression store (or turbulence induced by this process) increasing
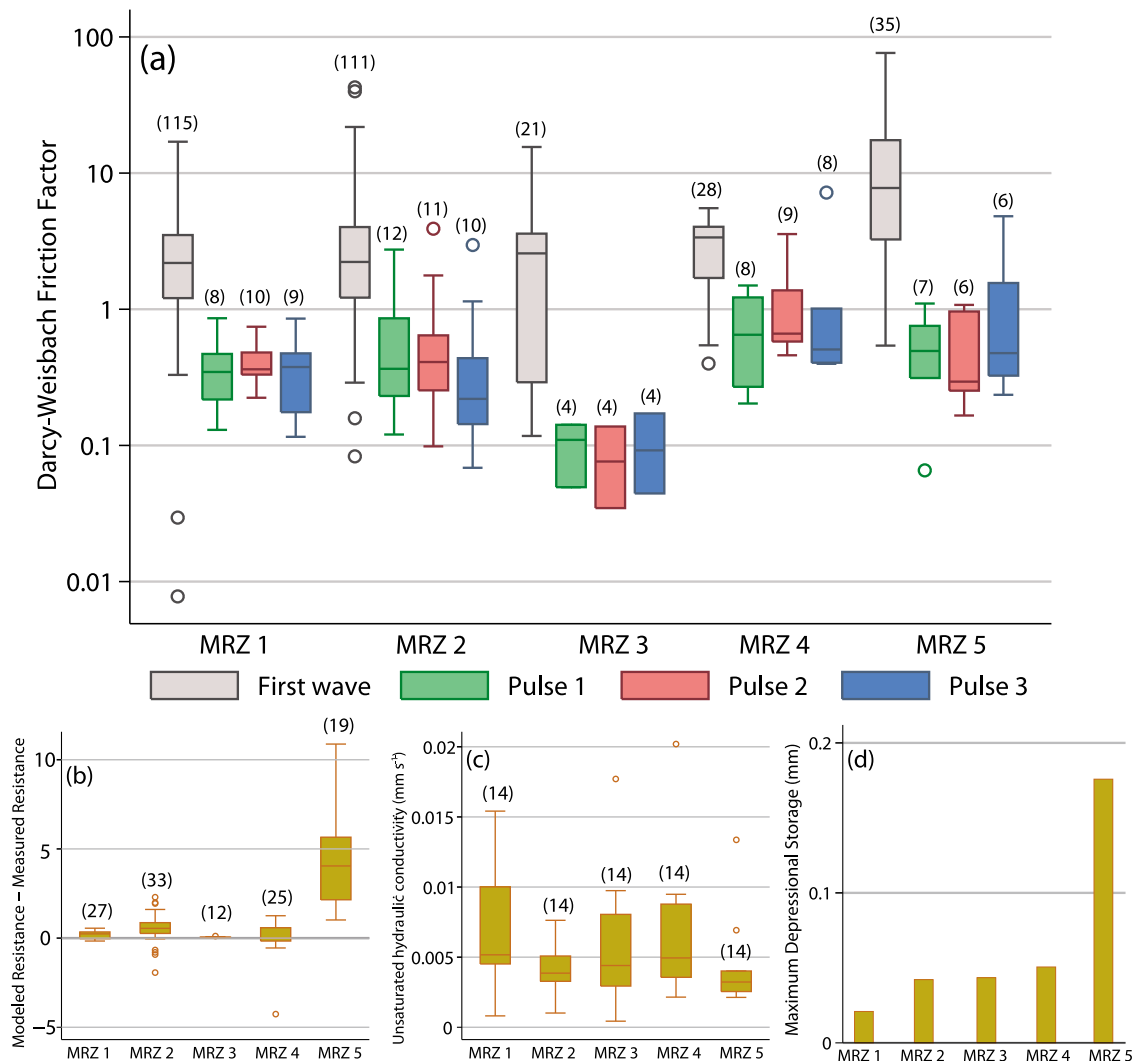
**Figure 11.** (a) Variation of *f* between pulses at each plot of the Del Prado hillslope, (b) variation of the difference between modeled resistance (using the empirical equations presented by *Smith et al.* [2010]) and measured resistance, (c) unsaturated hydraulic conductivity *k* (mm s$^{-1}$), and (d) maximum depressional storage at each plot of the Del Prado hillslope. For an explanation of a box plot see Figure 9.

the effective resistance to the first water wave. These results provide no direct evidence for this mechanism; indeed the pattern is inconsistent as the MRZ 4 plot showed the second largest surface depressional storage, yet was the closest-fitting model.

[55] An examination of measures of surface roughness used to predict *f* in Figure 10 found a systematic shift in the standard deviation of elevations from the first wave to the later dye pulses for the plots downslope of MRZ 3. This shift reduced the modeled flow resistance estimate at these locations, thereby counteracting the possible effect of the high depression storage at MRZ 4. It is clear that more research is required to untangle these effects and incorporate them into predictions of flow resistance.

## 6. A Conceptual Model to Quantify Hydrological Connectivity

[56] Several characteristics of hillslopes (and small catchments) must be incorporated in any quantitative anal-

ysis of hydrological connectivity. The distribution of travel times and the arrival of runoff at key points in the flow network will have a large influence on flood magnitudes in environments where transmission losses are high. This is affected by temporal structure of the rainfall event, spatial configuration of active runoff generating areas, distribution of flow path lengths, integration of flow paths (drainage structure), and routing velocity of overland flows.

[57] While compiling such a complete data set would prove impractical for most catchments, such information can be used to design modeling schemes which may identify relevant metrics. Classifying hillslope surfaces according to observed microtopography (using the morphological runoff zone framework of *Bracken and Kirkby* [2005]) provides a simple and reproducible methodology for upscaling resistance predictions to semiarid hillslopes. This is necessary to effectively integrate data sets from each of the components of the conceptual model identified here.

[58] A comparison of rainfall and runoff records suggests that antecedent moisture conditions before high-intensity
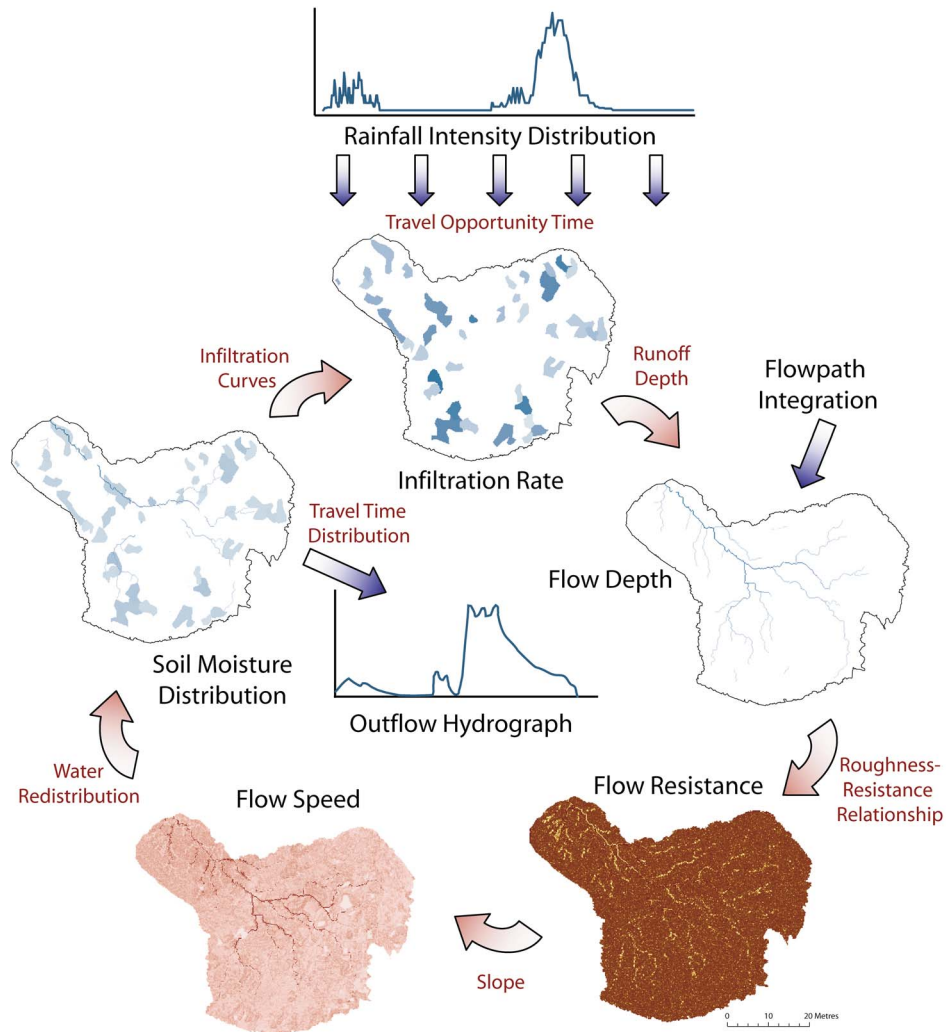
**Figure 12.** Summary of the conceptual model of dynamic hydrological connectivity over a semiarid hillslope outlined in this paper. Flow resistance and infiltration parameters interact through the redistribution of soil moisture and runoff to determine the runoff response to any given rainstorm.

rainfall pulses plays an important role, reducing losses to infiltration. This effect appears to be limited to runoff generation, having a negligible influence on routing velocities. However, the effect on runoff transfer is indirect and is established via flow depth-resistance relationships.

[59] Spatially and temporally variable flow resistance values are a key component of the conceptual model outlined in this paper, yet this is often neglected in models of hillslope hydrology. Spatial and temporal variations of both infiltration and flow resistance and the temporal distribution of rainfall intensities interact through the redistribution of soil moisture and runoff to determine catchment outflow and the scale dependency of runoff coefficients. This interaction is demonstrated for the Del Prado hillslope in Figure 12. Flow resistance varies with available runoff depth as determined by infiltration rates. In turn, infiltration rate is affected by soil moisture distribution, as determined by both rainfall inputs and horizontal moisture transfers controlled by resistance to flow. This interaction is responsible for the nonlinear runoff response observed on natural semiarid hillslopes, explaining not just the peak runoff but also the

total runoff amount (as a consequence of the limited "travel opportunity time" [*Aryal et al.*, 2003]). As such, the same degree of flexibility afforded to the modeling of infiltration rates (i.e., spatially variable, classified according to surface properties and time variable) should be applied to overland flow resistance predictions in the calculation of routing velocities to enable a more thoroughly quantitative and dynamic understanding of hydrological connectivity in semiarid environments.

[60] Relevant metrics of hydrological connectivity should thus be defined with this conceptual framework in mind. While section 4.3 demonstrated the importance of hillslope form in determining travel times, sections 4.4 and 4.5 highlighted the difficulty of estimating the required flow velocities, given the spatial and temporally variable nature of flow resistance. The probabilistic resistance-depth curves presented here can be easily incorporated into existing hydrological models. Where a flow depth has been determined, the predicted resistance distribution for that particular flow depth can be randomly sampled (from calculated percentiles) and a friction factor applied. Classifying each cell
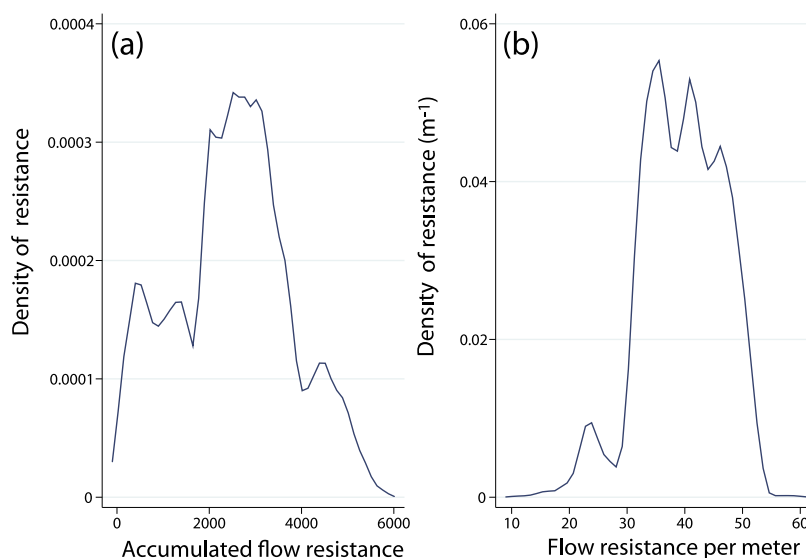
**Figure 13.** Example kernel density estimate showing the variation of (a) total flow resistance integrated over entire flow path (Epanechnikov kernel with a half width of 100) and (b) accumulated resistance per meter flow path length (half width 1) for the Del Prado hillslope. Calculated using a grid size of 50 mm and assuming a uniform flow depth of 2 mm.

using the MRZ framework allows different cells to access different curves and distributions of resistance predictions.

[61] Integration of the estimated flow resistance along the entire flow path length would identify both isolated and connected areas. This is demonstrated in Figure 13a for the simple case of a uniform flow depth of 2 mm and is analogous to the travel time distributions of Figure 8b. While the value itself has no physical meaning and is highly dependent on grid size, it represents a metric of connectivity to the hillslope outlet. Scaling this accumulated resistance by the path length (i.e., resistance per meter traveled) identifies relatively (dis)connected areas (Figure 13b) upon which local infiltration rates can be superimposed. Where areas of low infiltration rate coincide with areas of high transmission potential (low accumulated resistance per meter) hillslope outflow would more readily occur. The distribution of these values can be mapped easily across a hillslope. In this example, the initial rise to the left of the main peak (Figure 13b) represents the well-connected gully network that also connects early in Figure 8a.

[62] Eventually, dynamic feedback between runoff amounts and MRZ thresholds could be established (offering potential to represent effects of climate or land use change). This will allow examination of the interplay between hillslope morphology, rainfall characteristics and flow resistance and the resultant effect on flood generation over semiarid hillslopes (e.g., Figure 12).

## 7. Conclusions

[63] Dynamic hydrological connectivity on semiarid hillslopes arises from the interaction between the spatial distribution of infiltration rates and runoff transfer rates; metrics of dynamic connectivity should account for this. Representations of hillslope-scale connectivity must consider infiltration and resistance over the entire flow path of runoff generated at any point on the slope. Distributed estimates of infiltration rates and flow resistance are thus required alongside an appreciation of the overall hillslope form. The morphological runoff zone framework is proposed as a method for estimating spatial and temporal variations in flow resistance across hillslopes. It is recognized that these estimates, particularly their spatial structure within each MRZ, require further investigation. Further field experiments are needed to establish the absolute flow resistance values from rainfall simulation experiments and investigation of velocity correction factors. Moreover, the effect of vegetation on runoff connectivity must be established before any meaningful hillslope-scale model validation can take place.

[64] By definition, any metric of dynamic connectivity must move beyond the example of Figure 13 and continually reiterate resistance estimates throughout a storm event. The resistance-depth feedback mechanism identified in Figure 12 provides one realization of this. Further examination of interactions between infiltration rates, flow resistance and the temporal structure of rainfall intensities presents an opportunity to introduce a greater degree of quantification to the hydrological connectivity framework and provides insight into the controls on semiarid flood generation at the hillslope scale. Resistance-depth curves could be easily incorporated into existing hydrological models, providing a platform from which to develop such a quantified approach. Appropriate field experiments must be designed to inform modeling tools capable of investigating these interactions. This would ultimately improve our ability to predict the arrival time and size of initial flood waves and also flood volumes in arid and semiarid catchments, informing targeted management strategies to reduce the downstream impact of high-magnitude flood events.

development of the methodology and equipment; and Mike Kirkby, Rob Ferguson, Rich Hardy and anonymous reviewers for insights and thoughtful discussion.

# References

Abrahams, A. D., A. J. Parsons, and S.-H. Luk (1986), Field measurement of the velocity of overland flow using dye tracing, *Earth Surf. Processes Landforms*, *11*, 653–657, doi:10.1002/esp.3290110608.

Ali, G. A., and A. G. Roy (2009), Revisiting hydrologic sampling strategies for an accurate assessment of hydrologic connectivity in humid temperate systems, *Geogr. Compass*, *3*, 350–374, doi:10.1111/j.1749-8198.2008.00180.x.

Ambroise, B. (2004), Variable 'active' versus 'contributing' areas or periods: A necessary distinction, *Hydrol. Processes*, *18*, 1149–1155, doi:10.1002/hyp.5536.

Antoine, M., M. Javaux, and C. Bielders (2009), What indicators can capture runoff-relevant connectivity properties of the micro-topography at the plot scale?, *Adv. Water Resour.*, *32*, 1297–1310, doi:10.1016/j.advwatres.2009.05.006.

Aryal, S. K., R. G. Mein, and E. M. O'Loughlin (2003), The concept of effective length in hillslopes: Assessing the influence of climate and topography on the contributing area of catchments, *Hydrol. Processes*, *17*, 131–151, doi:10.1002/hyp.1137.

Berndtsson, R., and M. Larson (1987), Spatial variability of infiltration in a semi-arid environment, *J. Hydrol.*, *90*, 117–133, doi:10.1016/0022-1694(87)90175-2.

Bracken, L. J., and J. Croke (2007), The concept of connectivity and its application in geomorphology, *Hydrol. Processes*, *21*, 1749–1763, doi:10.1002/hyp.6313.

Bracken, L. J., and M. J. Kirkby (2005), Differences in hillslope runoff and sediment transport rates within two semi-arid catchments in southeast Spain, *Geomorphology*, *68*, 183–200, doi:10.1016/j.geomorph.2004.11.013.

Bracken, L. J., N. J. Cox, and J. Shannon (2008), The relationship between rainfall inputs and flood generation in south-east Spain, *Hydrol. Processes*, *22*, 683–696, doi:10.1002/hyp.6641.

Brunsden, D. (1993), Barriers to geomorphological change, in *Landscape Sensitivity*, edited by D. S. G. Thomas and R. J. Allison, pp. 7–12, John Wiley, Chichester, U. K.

Bull, L. J., M. J. Kirkby, J. Shannon, and J. M. Hooke (2000), The impact of rainstorms on floods in ephemeral channels in SE Spain, *Catena*, *38*, 191–209, doi:10.1016/S0341-8162(99)00071-5.

Bull, L. J., M. J. Kirkby, J. Shannon, and H. D. Dunsford (2003), Predicting hydrologically similar surfaces (HYSS) in semi-arid environments, *Adv. Environ. Monit. Model.*, *1*, 1–26.

Cammeraat, E. L. H. (2004), Scale dependent thresholds in hydrological and erosion response of a semi-arid catchment in southeast Spain, *Agric. Ecosyst. Environ.*, *104*, 317–332, doi:10.1016/j.agee.2004.01.032.

Costa, J. E. (1987), A comparison of the largest rainfall-runoff floods in the United States and the People's Republic of China and the world, *J. Hydrol.*, *96*, 101–115, doi:10.1016/0022-1694(87)90146-6.

Cox, N. J. (2006), Assessing agreement of measurements and predictions in geomorphology, *Geomorphology*, *76*, 332–346, doi:10.1016/j.geomorph.2005.12.001.

Cox, N. J. (2007), Kernel estimation as a basic tool for geomorphological data analysis, *Earth Surf. Processes Landforms*, *32*, 1902–1912, doi:10.1002/esp.1518.

Croke, J., and S. Mockler (2001), Gully initiation and road-to-stream linkage in a forested catchment, south eastern Australia, *Earth Surf. Processes Landforms*, *26*, 205–217, doi:10.1002/1096-9837(200102)26:2<205::AID-ESP168>3.0.CO;2-G.

de Lima, J. L. M. P., V. P. Singh, and M. I. P. de Lima (2003), The influence of storm movement on water erosion: Storm direction and velocity effects, *Catena*, *52*, 39–56, doi:10.1016/S0341-8162(02)00149-2.

Devito, K., I. Creed, T. Gan, C. Mendoza, R. Petrone, U. Silins, and B. Smerdon (2005), A framework for broad-scale classification of hydrologic response units on the boreal plain: Is topography the last thing to consider?, *Hydrol. Processes*, *19*, 1705–1714, doi:10.1002/hyp.5881.

Di Domenico, A., G. Laguardia, and M. Fiorentino (2007), Capturing critical behaviour in soil moisture spatio-temporal dynamics, *Adv. Water Resour.*, *30*, 543–554, doi:10.1016/j.advwatres.2006.04.007.

Fitzjohn, C., J. L. Ternan, and A. G. Williams (1998), Soil moisture variability in a semi-arid gully catchment: Implications for runoff and erosion control, *Catena*, *32*, 55–70, doi:10.1016/S0341-8162(97)00045-3.

Flügel, W. A. (1995), Delineating hydrological response units by geographical information system analyses for regional hydrological modeling using PRMS/MMS in the drainage basin of the river Brol, Germany, *Hydrol. Processes*, *9*, 423–436, doi:10.1002/hyp.3360090313.

Gomi, T., R. C. Sidle, S. Miyata, K. Kosugi, and Y. Onda (2008), Dynamic runoff connectivity of overland flow on steep forested hillslopes: Scale effects and runoff transfer, *Water Resour. Res.*, *44*, W08411, doi:10.1029/2007WR005894.

Grayson, R. B., G. Blöschl, A. W. Western, and T. A. McMahon (2002), Advances in the use of observed spatial patterns of catchment hydrological response, *Adv. Water Resour.*, *25*, 1313–1334, doi:10.1016/S0309-1708(02)00060-X.

Harrell, F. E. (2001), *Regression Modeling Strategies*, Springer, New York.

Hooke, J. M., and J. M. Mant (2000), Geomorphological impacts of a flood event on ephemeral channels in SE Spain, *Geomorphology*, *34*, 163–180, doi:10.1016/S0169-555X(00)00005-2.

Hopp, L., and J. J. McDonnell (2009), Connectivity at the hillslope scale: Identifying interactions between storm size, bedrock permeability, slope angle and soil depth, *J. Hydrol.*, *376*, 378–391, doi:10.1016/j.jhydrol.2009.07.047.

Horton, R. E. (1945), Erosional development of streams and their drainage basins: Hydrophysical approach to quantitative morphology, *Geol. Soc. Am. Bull.*, *56*, 275–370, doi:10.1130/0016-7606(1945)56[275:EDOSAT]2.0.CO;2.

Karvonen, T., H. Koivusalo, M. Jauhiainen, J. Palko, and K. Weppling (1999), A hydrological model for predicting runoff from different land-use areas, *J. Hydrol.*, *217*, 253–265, doi:10.1016/S0022-1694(98)00280-7.

Kirkby, M. J., L. J. Bracken, and J. Shannon (2005), The influence of rainfall distribution and morphological factors on runoff delivery from dryland catchments in SE Spain, *Catena*, *62*, 136–156, doi:10.1016/j.catena.2005.05.002.

Kuhn, N., and A. Yair (2004), Spatial distribution of surface conditions and runoff generation in small arid watersheds, Zin Valley Badlands, Israel, *Geomorphology*, *57*, 183–200, doi:10.1016/S0169-555X(03)00102-8.

Lane, S. N., C. J. Brooks, M. J. Kirkby, and J. Holden (2004), A network-index-based version of TOPMODEL for use with high-resolution digital topographic data, *Hydrol. Processes*, *18*, 191–201, doi:10.1002/hyp.5208.

Lawrence, D. S. L. (1997), Macroscale surface roughness and frictional resistance in overland flow, *Earth Surf. Processes Landforms*, *22*, 365–382, doi:10.1002/(SICI)1096-9837(199704)22:4<365::AID-ESP693>3.0.CO;2-6.

Lehmann, P., C. Hinz, G. McGrath, H. J. Tromp-van Meervold, and J. J. McDonnell (2007), Rainfall threshold for hillslope outflow: An emergent property of flow pathway connectivity, *Hydrol. Earth Syst. Sci.*, *11*, 1047–1063, doi:10.5194/hess-11-1047-2007.

Li, X. Y., A. González, and A. Solé-Benet (2005), Laboratory methods for the estimation of infiltration rate of soil crusts in the Tabernas desert badlands, *Catena*, *60*, 255–266, doi:10.1016/j.catena.2004.12.004.

Lin, L. I.-K. (1989), A concordance correlation coefficient to evaluate reproducibility, *Biometrics*, *45*, 255–268, doi:10.2307/2532051.

Lin, L. I.-K. (2000), A note on the concordance correlation coefficient, *Biometrics*, *56*, 324–325.

McDonnell, J. J., et al. (2007), Moving beyond heterogeneity and process complexity: A new vision for watershed hydrology, *Water Resour. Res.*, *43*, W07301, doi:10.1029/2006WR005467.

Michaelides, K., and J. Wainwright (2002), Modeling the effects of hillslope-channel coupling on catchment hydrological response, *Earth Surf. Processes Landforms*, *27*, 1441–1457, doi:10.1002/esp.440.

Morgan, R. P. C., J. N. Quinton, R. E. Smith, G. Govers, J. W. A. Poesen, K. Auerswald, G. Chisci, D. Torri, and M. E. Styczen (1998), The European soil erosion model (EUROSEM): A dynamic approach for predicting sediment transport from fields and small catchments, *Earth Surf. Processes Landforms*, *23*, 527–544, doi:10.1002/(SICI)1096-9837(199806)23:6<527::AID-ESP868>3.0.CO;2-5.

Morin, J., and Y. Benyamini (1977), Rainfall infiltration into bare soils, *Water Resour. Res.*, *13*, 813–817, doi:10.1029/WR013i005p00813.

Mueller, E. N., J. Wainwright, and A. Parsons (2007), Impact of connectivity on the modeling of overland flow within semiarid shrubland environments, *Water Resour. Res.*, *43*, W09412, doi:10.1029/2006WR005006.

Nash, J. E. (1957), The form of the instantaneous unit hydrograph, *Bull. Int. Assoc. Sci. Hydrol.*, *45*, 114–121.

Parsons, A. J., A. D. Abrahams, and J. Wainwright (1994), On determining resistance to interrill overland flow, *Water Resour. Res.*, *30*, 3515–3521, doi:10.1029/94WR02176.

Planchon, O., N. Silvera, R. Giménez, D. Favis-Mortlock, J. Wainwright, Y. Lebissonnais, and G. Govers (2005), An automated salt-tracing gauge for flow-velocity measurement, *Earth Surf. Processes Landforms*, *30*, 833–844, doi:10.1002/esp.1194.

Reaney, S. M. (2008), The use of agent-based modeling techniques in hydrology: Determining the spatial and temporal origin of channel flow in semi-arid catchments, *Earth Surf. Processes Landforms*, *33*, 317–327, doi:10.1002/esp.1540.

Reaney, S. M., L. J. Bracken, and M. J. Kirkby (2007), Use of the connectivity of runoff model (CRUM) to investigate the influence of storm characteristics on runoff generation and connectivity in semi-arid areas, *Hydrol. Processes*, *21*, 894–906, doi:10.1002/hyp.6281.

Rodríguez-Iturbe, I., and J. Valdès (1979), The geomorphic structure of hydrologic response, *Water Resour. Res.*, *15*, 1409–1420, doi:10.1029/WR015i006p01409.

Schick, A. P. (1988), Hydrologic aspects of floods in extreme arid environments, in *Flood Geomorphology*, edited by V. R. Baker, R. C. Kochel, and P. C. Patton, pp. 189–203, John Wiley, New York.

Schröder, B. (2006), Pattern, process and function in landscape ecology and catchment hydrology—How can quantitative landscape ecology support predictions in ungauged basins?, *Hydrol. Earth Syst. Sci.*, *10*, 967–979, doi:10.5194/hess-10-967-2006.

Sharma, K. D., M. Menenti, J. Huygen, and P. C. Fernandez (1996), Distributed numerical rainfall-runoff modeling in an arid region using Thematic Mapper data and a geographical information system, *Hydrol. Processes*, *10*, 1229–1242, doi:10.1002/(SICI)1099-1085(199609)10:9<1229::AID-HYP381>3.0.CO;2-Y.

Sherman, L. K. (1932), Streamflow from rainfall by unit-graph method, *Eng. News Record*, *108*, 501–505.

Sidle, R. C., S. Noguchi, Y. Tsuboyama, and K. Laursen (2001), A conceptual model of preferential flow systems in forested hillslopes: Evidence of self-organisation, *Hydrol. Processes*, *15*, 1675–1692, doi:10.1002/hyp.233.

Sivapalan, M. (2005), Pattern, process and function: Elements of a unified theory of hydrology at the catchment scale, in *Encyclopedia of Hydrological Sciences*, edited by M. G. Anderson, pp. 193–219, John Wiley, Chichester, U. K.

Smart, G. M., M. J. Duncan, and J. M. Walsh (2002), Relatively rough flow resistance equations, *J. Hydraul. Eng.*, *128*(6), 568–578, doi:10.1061/(ASCE)0733-9429(2002)128:6(568).

Smith, M. W. (2009), Overland flow resistance and flood generation in semi-arid environments, Ph.D. thesis, 373 pp., Durham Univ., Durham, U. K.

Smith, M. W., N. J. Cox, and L. J. Bracken (2007), Applying flow resistance equations to overland flows, *Prog. Phys. Geogr.*, *31*(4), 363–387, doi:10.1177/0309133307081289.

Smith, M. W., N. J. Cox, and L. J. Bracken (2010), Terrestrial laser scanning soil surfaces: A field methodology to examine soil surface roughness and overland flow hydraulics, *Hydrol. Processes.*, doi:10.1002/hyp.7871, in press.

Smith, T. R., and F. P. Bretherton (1972), Stability and the conservation of mass in drainage basin evolution, *Water Resour. Res.*, *8*, 1506–1529, doi:10.1029/WR008i006p01506.

Tetzlaff, D., C. Soulsby, P. J. Bacon, A. F. Youngson, C. Gibbins, and I. A. Malcom (2007), Connectivity between landscapes and riverscapes—A unifying theme in integrating hydrology and ecology in catchment science?, *Hydrol. Processes*, *21*, 1385–1389, doi:10.1002/hyp.6701.

Troch, P. A., G. A. Carrillo, I. Heidbüchel, S. Rajagopal, M. Switanek, T. H. M. Volkmann, and M. Yaegar (2009), Dealing with landscape heterogeneity in watershed hydrology: A review of recent progress toward new hydrological theory, *Geogr. Compass*, *3*, 375–392, doi:10.1111/j.1749-8198.2008.00186.x.

Tromp-van Meerveld, H. J., and J. J. McDonnell (2006), Threshold relations in subsurface stormflow: 2. The fill and spill hypothesis, *Water Resour. Res.*, *42*, W02411, doi:10.1029/2004WR003800.

Turnbull, L., J. Wainwright, and R. E. Brazier (2008), A conceptual framework for understanding semi-arid land degradation: Ecohydrological interactions across multiple-space and time scales, *Ecohydrology*, *1*, 23–34, doi:10.1002/eco.4.

van de Giesen, N. C., T. J. Stomph, and N. de Ridder (2000), Scale effects of Hortonian overland flow and rainfall-runoff dynamics in a West African catena landscape, *Hydrol. Processes*, *14*, 165–175, doi:10.1002/(SICI)1099-1085(200001)14:1<165::AID-HYP920>3.0.CO;2-1.

Van Deursen, W. P. A., and C. G. Wesseling (1992), The PCRaster package, Dep. of Phys. Geogr., Utrecht Univ., Utrecht, Netherlands.

Wainwright, J., and A. J. Parsons (2002), The effect of temporal variations in rainfall on scale dependency in runoff coefficients, *Water Resour. Res.*, *38*(12), 1271, doi:10.1029/2000WR000188.

Western, A. W., G. Blöschl, and R. B. Grayson (1998), How well do indicator variograms capture the spatial connectivity of soil moisture?, *Hydrol. Processes*, *12*, 1851–1868, doi:10.1002/(SICI)1099-1085(19981015)12:12<1851::AID-HYP670>3.0.CO;2-P.

Western, A. W., G. Blöschl, and R. B. Grayson (2001), Towards capturing hydrologically significant connectivity in spatial patterns, *Water Resour. Res.*, *37*(1), 83–97, doi:10.1029/2000WR900241.

Yair, A., and A. Kossovsky (2002), Climate and surface properties: Hydrological response of small arid and semi-arid watersheds, *Geomorphology*, *42*, 43–57, doi:10.1016/S0169-555X(01)00072-1.

Yair, A., and N. Raz-Yassif (2004), Hydrological processes in a small arid catchment: Scale effects of rainfall and slope length, *Geomorphology*, *61*, 155–169, doi:10.1016/j.geomorph.2003.12.003.

Zhang, R. (1997), Determination of soil sorptivity and hydraulic conductivity from the disk infiltrometer, *Soil Sci. Soc. Am. J.*, *61*, 1024–1030, doi:10.2136/sssaj1997.03615995006100040005x.

L. J. Bracken and N. J. Cox, Department of Geography, Durham University, Durham DH1 3LE, UK.

M. W. Smith, Institute of Geography and Earth Sciences, Aberystwyth University, Aberystwyth SY23 3DB, UK. (mark.smith@aber.ac.uk)